

YOUNG SUPERNOVAE AS EXPERIMENTAL SITES TO STUDY ELECTRON ACCELERATION MECHANISM

KEIICHI MAEDA¹

Draft version September 21, 2018

ABSTRACT

Radio emissions from young supernovae ($\lesssim 1$ year after the explosion) show a peculiar feature in the relativistic electron population at a shock wave, where their energy distribution is steeper than typically found in supernova remnants (SNRs) and than the prediction from the standard diffusive shock acceleration (DSA) mechanism. This is especially established for a class of stripped envelope supernovae (SNe I Ib/Ib/Ic) where a combination of high shock velocity and low circumstellar material (CSM) density makes it easier to derive the intrinsic energy distribution than in other classes of SNe. We suggest that this apparent discrepancy reflects the situation that the low energy electrons before accelerated by the DSA-like mechanism are responsible for the radio synchrotron emission from young SNe, and that studying young SNe sheds light on the still-unresolved electron injection problem in the acceleration theory of cosmic rays. We suggest that electron's energy distribution could be flattened toward the high energy, most likely around 100 MeV, which marks a transition from inefficient to efficient acceleration. Identifying this feature will be a major advance in understanding the electron acceleration mechanism. We suggest two further probes: (1) *mm/sub-mm* observations in the first year after the explosion, and (2) X-ray observations at about 1 year and thereafter. We show that these are reachable by *ALMA* and *Chandra* for nearby SNe.

Subject headings: Acceleration of particles – radiation mechanism: non-thermal – shock waves – supernovae: general – supernovae: individual: SN 2011dh

1. INTRODUCTION

The most promising cosmic-ray acceleration mechanism involves a strong shock wave. In the standard DSA scenario (Fermi 1949; Blandford & Ostriker 1978; Bell 1978), particles acquire energy through multiple shock crossings between upstream and downstream. Studying two acceleration sites – young SNe and evolved SNRs – provides a seemingly controversial result. Young SNe expanding into CSM launch a strong shock wave. The shock wave generates/amplifies the magnetic field and accelerates electrons (Chevalier 1998; Chevalier & Fransson 2006b), as is similar to SNRs. Stripped-envelope SNe, or SNe I Ib/Ib/Ic, are well-studied in *cm* wavelengths (e.g., Chevalier & Fransson 2006b; Soderberg et al. 2012; Krauss et al. 2012; Maeda 2012a,b; Horesh et al. 2012). They are characterized by a combination of high shock velocity and relatively low CSM density, thus providing an ideal site to study the intrinsic energy distribution of relativistic electrons, less affected by absorption or cooling than other classes of SNe (Chevalier 1998; Chevalier & Fransson 2006b). The intrinsic power law index is typically found to be $p \sim 3$ (where $N(E)/dE \propto E^{-p}$) (Chevalier & Fransson 2006b), not as efficient as predicted by the DSA mechanism ($p = 2$: Blandford & Ostriker 1978; Bell 1978; Ellison et al. 2000; Morlino & Caprioli 2012). On the other hand, the *cm* emission from SNRs is generally consistent with the DSA prediction (e.g., Bamba et al. 2003; Uchiyama et al. 2007).

In this paper, we suggest that this apparent discrepancy indeed provides a strong hint to understanding how

electrons are injected into the DSA mechanism (§2). We suggest a scenario which explains the different properties of the radio-emitting electrons in a unified scheme. Our interpretation provides (at least) two observational signatures: (1) *mm* emissions in the first year after the explosion (§3), and (2) X-ray synchrotron emissions at about 1 years after the explosion and thereafter (§4). The paper is closed in §5 with concluding remarks.

2. ELECTRON ACCELERATION TOWARD THE DSA MECHANISM

A major issue remains on the acceleration of electrons. For the standard DSA mechanism (Fermi 1949; Blandford & Ostriker 1978; Bell 1978) to work effectively, the particles must already have enough kinetic energy (at least $\gamma \gtrsim 200$ for electrons in SNe I Ib/Ib/Ic, where γ is the Lorentz factor; see below). Numerical simulations predict that the energy distribution in the high energy regime follows the linear theory of DSA (with $p \sim 2$) while in the lower energy it can be steeper (Ellison et al. 2000; Morlino & Caprioli 2012). First, let us provide a simple argument on at which energy the electrons have a sufficient energy to be accelerated by the efficient DSA-like mechanism. The width of the collisionless shock wave can be approximated by the gyro radius of downstream *thermal* protons, while the mean free path of relativistic electrons can be approximated by the gyro radius of the *relativistic* electrons. Then, the condition that the electron's mean free path exceeds the shock wave width is expressed as

$$E \gtrsim m_e c^2 \left(\frac{m_p}{m_e} \right) \left(\frac{V}{c} \right) \sim 100 \text{ MeV (i.e., } \gamma \gtrsim 200 \text{)}, \quad (1)$$

where $V \sim 0.1c$ is the shock wave velocity typically seen in young SNe I Ib/Ib/Ic. The same criterion is $\gamma \gtrsim 20$ for

¹ Kavli Institute for the Physics and Mathematics of the Universe (Kavli-IPMU), University of Tokyo, 5-1-5 Kashiwanoha, Kashiwa, Chiba 277-8583, Japan; keiichi.maeda@ipmu.jp

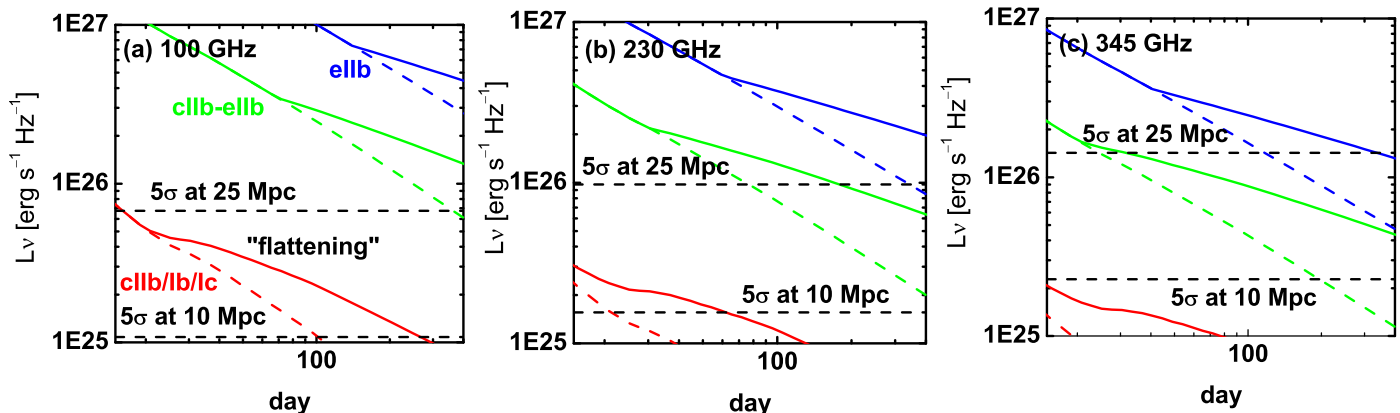


FIG. 1.— Examples of multi frequency light curves of SN-CSM interaction. Our reference model (‘cIIb/Ib/Ic’ shown in red) is the one which fits to the spectra and light curves of SN cIIb 2011dh in *cm* wavelengths, where $A_* = 4$. For the same model, the one with the spectral flattening at $\gamma = 200$ and without it are shown by solid and dashed, respectively. We also examine models where only the CSM density is changed, to $A_* = 200$ (‘eIIb’) and $A_* = 50$ (‘cIIb-eIIb’). The 5σ detection limits in the continuum observation mode of *ALMA* with an exposure of one hour in each Band 3, 6, 7 are shown by dashed lines.

SNRs with $V \sim 0.01c$. This assumes the Bohm limit for the strength of random magnetic field turbulence which is likely realized in the SN-CSM interaction, but if it is not the case the above criterion will go down. Above this energy, electrons can experience the whole compression ($r = 4$), and therefore $p = (r + 2)/(r - 1) = 2$ in the test particle limit. On the other hand, the acceleration of electrons below this energy can be totally different: Either the non-DSA pre-acceleration mechanism dominates, or these electrons are partly accelerated by the DSA in the non-linear regime (Ellison et al. 2000) where the subshock compression ratio is reduced by the feedback of the proton acceleration (Tatischeff 2009). These processes expected for these low energy electrons could result in a steep distribution with $p > 2$.

Now, we compare this critical energy scale to the energy of radio-synchrotron emitting electrons (in *cm* wavelengths). The electron’s energy and the corresponding synchrotron emission frequency are connected by

$$\gamma \sim 80\nu_{10}^{0.5} B^{-0.5}, \quad (2)$$

where $\nu \equiv 10^{10}\nu_{10}$ Hz, and B is the magnetic field strength behind the shock in gauss. Observationally, $B \sim 1$ G in SNe I Ib/Ic and $B \sim 100\mu$ G in evolved SNRs. We note this is consistent with an expectation from equipartition: In equipartition ($B^2/4\pi \equiv \epsilon_B \rho_{\text{CSM}} V^2$) and for the same reference value of $\epsilon_B \sim 0.1$, we expect $B \sim 1$ G for young SNe ($n_{\text{CSM}} \sim 10^6 \text{ cm}^{-3}$ and $V \sim 0.1c$) and $B \sim 100\mu$ G for SNRs ($n_{\text{ISM}} \sim 1 \text{ cm}^{-3}$ and $V \sim 0.01c$). At 10 GHz typical of *cm* wavelengths, electrons’ energy responsible to the emission is $\gamma \sim 80$ in SNe I Ib/Ic and $\gamma \sim 8000$ in SNRs.

Following the above estimate, it is clear that the electrons emitting in *cm* wavelengths are totally in different energy regimes in young SNe and SNRs. The electrons’ energy responsible for the radio emission is certainly much above the DSA requirement for SNRs, so they are likely efficiently accelerated. On the other hand,

the radio-emitting electrons in young SNe unlikely satisfy the efficient DSA condition, i.e., the electrons do not feel the shock wave as infinitesimal discontinuity. We suggest this is a reason why different intrinsic slopes are obtained for young SNe and SNRs.

This interpretation offers a unique opportunity to study the electron acceleration mechanism, or the injection problem, through the SN-CSM interaction signals from young SNe. Our scenario predicts that the flattening of the intrinsic electron spectrum should take place above the energy currently probed in *cm* wavelengths. We propose two methods to further probe this issue using currently operating observatories: (1) *mm* observations (e.g., *ALMA*) and (2) X-ray observations (e.g., *Chandra*).

3. MM/SUB-MM EMISSION (E.G., *ALMA*)

At 100 GHz, the corresponding Lorentz factor of the synchrotron emitting electrons is $\gamma \sim 250$ for $B \sim 1$ G, which is the energy range in which the flattening could already happen announcing the possible transition from inefficient to efficient electron acceleration (§2). Figures 1 and 2 show an example of expected multi-band light curves in the *ALMA* bands, and the predicted spectral evolution for the same models. The model has been constructed through standard formalisms (Fransson & Björnsson 1998; Björnsson & Fransson 2004), and fits well to the multi band radio light curves of nearby SN I Ib 2011dh in 1.4 – 36 GHz (see Maeda 2012a, for the model details). Here, we include the effect of the spectral flattening (at γ_{fl}), while fixing all the other parameters as calibrated for SN 2011dh. We fix $\gamma_{\text{fl}} = 200$, and $p = 3$ and $p = 2$ below and above γ_{fl} . The inclusion of the spectral flattening does not affect the properties in *cm* wavelengths.

This model is shown in the figure as ‘cIIb/Ib/Ic’. We assume a steady-state wind for the CSM density as $\rho_{\text{CSM}} = 5 \times 10^{11} A_* r^{-2} \text{ g cm}^{-3}$ (r is the distance from the progenitor in *cm*), and we adopt $A_* = 4$ for SN I Ib 2011dh (Soderberg et al. 2012; Maeda 2012a). The

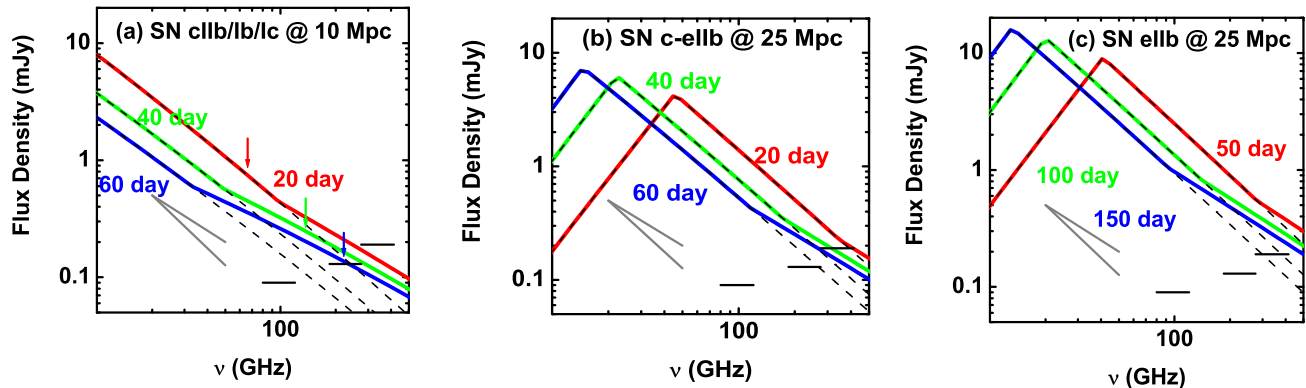


FIG. 2.— The spectral evolution of the model shown in Figure 1 (with $\gamma_H = 200$) at different epochs. The characteristic synchrotron cooling frequency is indicated by arrows for each snapshot for the model with $A_* = 4$ (‘cIIb/Ib/Ic’). For the other models, the cooling frequency is below the frequency range shown here. In each snapshot, a dashed curve is for the model without flattening. On the left-bottom corner, the power law behaviors are illustrated for the cooling-dominated synchrotron spectrum with $p = 3$ (derived in *cm* observations for a majority of SNe cIIb/Ib/Ic) and $p = 2$ (expected above the spectral flattening energy). The *ALMA* 5σ continuum sensitivities with an exposure of one hour are shown by black solid line in each band.

stripped-envelope SNe (IIb/Ib/Ic) are characterized by the absence/weakness of lines from particular elements in the optical maximum-light spectra (Filippenko et al. 1993; Filippenko 1997): Weak H lines in SNe IIb, (generally) absence of H lines in SNe Ib, and neither H nor He in SNe Ic. The origin of this difference is generally interpreted as a different amount of envelope stripped off during the hydrostatic evolutionary phase (Nomoto et al. 1993; Woosley et al. 1994). SNe IIb are (sometimes) further sub-divided into SNe eIIb (‘extended’) and SNe cIIb (‘compact’) (Chevalier & Soderberg 2010). SNe eIIb, cIIb, Ib/Ic are then linked to the different size of the progenitor envelope, where SNe eIIb are believed to come from a Red Supergiant (RSG) while SNe Ib/c are from a compact Wolf-Rayet (WR) (Chevalier & Soderberg 2010). Their different properties in radio wavelengths can be interpreted as mainly controlled by different CSM density rather than the SN properties (Maeda 2012b)², where the CSM is as dense as $A_* \sim 200$ for SNe eIIb (Fransson, Lundqvist, & Chevalier 1996; Fransson & Björnsson 1998), while it is less dense in SNe cIIb/Ib/Ic ($A_* \lesssim 10$) (Chevalier & Fransson 2006b). To take into account this variation, we also investigate SNe with more dense CSM, named ‘eIIb’ ($A_* = 200$) and a transitional case ‘cIIb-eIIb’ ($A_* = 50$). Note that even with $A_* = 200$, the free-free absorption is estimated to be negligible at ~ 100 GHz unlike in the *cm* wavelengths (Chevalier et al. 2006a), highlighting another useful nature of the high frequency observation – the transparency even for SNe within moderately high-density environments (e.g., SNe eIIb, IIp).

The spectral flattening in the electron energy distribution results in the flattening in the synchrotron spectrum. In light curves this is seen as a flattening in the decay

rate, which takes place first in the higher frequency then eventually in the lower frequency. For denser CSM the transition is further delayed and the large luminosity is attained due to the higher magnetic field content and higher relativistic electron density for denser CSM.

The model curves are compared to the 5σ detection limit in the continuum observation mode of *ALMA* with one-hour exposure in each band (Brown et al. 2004).³ Figure 1 shows that *ALMA* can detect the synchrotron signal from nearby SNe, and that the possible spectral fattening can be investigated. If $\gamma_H \sim 200$ as in our reference value (§2), this will be clearly identified in 100 – 345 GHz. For the Cycle-1 *ALMA* and an exposure of one hour, this is reachable for typical SNe cIIb/Ib/Ic up to ~ 10 Mpc, and to ~ 25 Mpc or even more for SNe eIIb and the intermediate case. For the larger value of γ_H , the beginning of this light curve flattening is delayed at the lower flux level.

Figure 2 shows the evolution of the synthesized spectrum as a function of time, for $\gamma_H = 200$. The spectral break frequency (corresponding to γ_H) moves toward the lower frequency as time goes by. The break appears within the *ALMA* bands at $\sim 20 - 100$ day, and later enters into the lower frequency bands. Thus, the multi-epoch follow-up is crucial, and coordinated follow up in *cm* wavelengths is strongly encouraged.

In these models, the synchrotron cooling is the dominant process in the energy range of interest here (Maeda 2012a). The cooling frequency evolves toward the higher energy. For the ‘cIIb’ model, initially it is below the *ALMA* bands, and later moves into the *ALMA* bands and even to the higher energy. This evolution is in the opposite direction to the one caused by the intrinsic spectral flattening, thus these two effects are distinguishable. It will give an independent estimate of the magnetic field

² Peak radio date and luminosity of SNe IIb/Ib/Ic follow the expectation in which CSM density is varied while the similar explosion properties are applied (Maeda 2012b).

³ We have used the Cycle 1 *ALMA* Observing Tool for the sensitivity calculation (<http://www.almaobservatory.org/>).

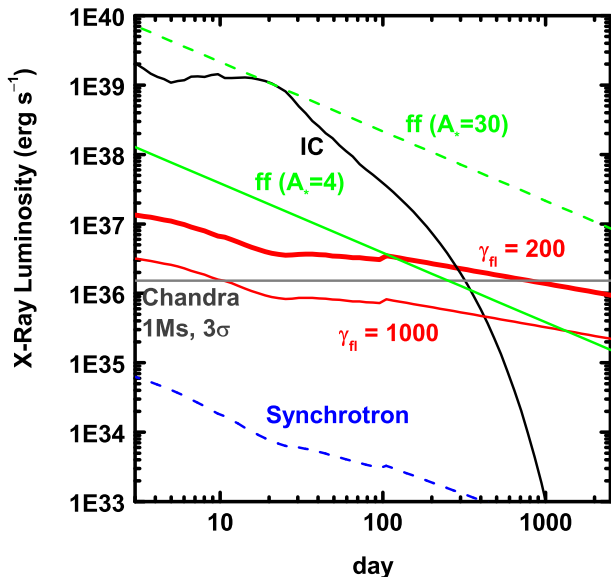


FIG. 3.— Predicted long-term X-ray light curve of SN 2011dh, including the effect of the possible spectral flattening. The model is the same with ‘cIIb’ model ($A_* = 4$) adopted from Maeda (2012a). The IC (black) is from the same model which fits the observed X-ray light curve by the IC (Maeda 2012a). The contribution from the free-free emission is shown by green, where the one with $A_* = 4$ (solid) is our reference model while the other with $A_* = 30$ (dashed) is the high density CSM model to account for the early X-ray emission by the free-free emission. The ‘original’ synchrotron X-ray emission is shown by blue dashed line. The synchrotron X-ray emission with the spectral flattening is shown by red solid lines, with $\gamma_{ff} = 200$ (thick) and $\gamma_{ff} = 1000$ (thin). At $\sim 10 - 100$ days, the synchrotron X-ray light curve shows slight suppression from the expected power law behavior due to an additional IC cooling. The 3σ detection limit of Chandra X-ray Observatory with an exposure of 1 Ms is shown by gray: Here, we scaled the detection limit obtained for SN 2011fe (Margui et al. 2012) to the distance to SN 2011dh and to the exposure of 1 Ms (assuming the Poisson-noise dominated).

strength through the relation $t \sim 110\nu_{10}^{-0.5}B^{-1.5}$ days, providing a rare case to test different scenarios for magnetic field generation/amplification.

4. X-RAY EMISSION (E.G., CHANDRA)

Another suggestion for the spectral flattening is to look into a late-time X-ray property (see also Chevalier & Fransson 2006b). Figure 3 shows an expected X-ray light curve evolution (νL_ν at ~ 1 keV). This model assumes an additional low energy relativistic electron population at $\gamma \lesssim 50$ to account for the X-ray luminosity at $\lesssim 40$ day by the Inverse Compton (IC) scattering, together with the power-law synchrotron-emitting electrons at $\gamma \gtrsim 50$. For the IC, we assume that the SN bolometric light curve follows the ^{56}Co decay after 100 days. This would overestimate the IC scattering effect there, so the IC contribution could decrease more quickly than shown in Figure 3 after 100 days. In addition to this reference model, Maeda (2012a) provided another possibility, where the CSM density is as high as $A_* \sim 30$ and the X-ray is dominated by the free-free emission from the thermal electrons (see also Campana & Immler 2012; Sasaki & Ducci 2012). While

Maeda (2012a) (see also Soderberg et al. 2012) preferred the low-density solution in view of a connection to other SNe Ib/c, the early-phase observation of SN 2011dh itself did not discriminate these two possibilities.

The synchrotron contribution is small as compared to other mechanisms if we extrapolate the intrinsic electron energy distribution derived for the radio emitting electrons ($\gamma \sim 100$) to the X-ray synchrotron emitting electrons (i.e., without the flattening). With the spectral flattening the synchrotron X-ray is enhanced, and can dominate the free-free emission at $\gtrsim 100$ days if $\gamma_{ff} \sim 200$ (if $A_* = 4$). It further dominates the IC X-ray at $\gtrsim 300$ days. On the other hand, the free-free always dominates the X-ray emission if the CSM density is as high as $A_* = 30$. This provides a test for the origin of the X-ray emission from SN 2011dh. If the early-phase X-ray was due to the high density CSM and the free-free emission, then the late-phase X-ray luminosity should stay as luminous as 10^{37} erg s^{-1} even at a few years after the explosion. Otherwise, it should be below $\sim 10^{36}$ erg s^{-1} .

The free-free emission follows the temporal evolution of $\nu L_{ff} \propto t^{-1}$ (Chevalier et al. 2006a; Chevalier & Fransson 2006b). The synchrotron X-ray is in the cooling regime, and roughly follows $\nu L_{syn} \propto t^{-0.8}$ without the flattening (Chevalier & Fransson 2006b; Maeda 2012b). With the flattening at $\gamma_{ff} = 200$, the synchrotron X-ray emitting electrons are above this energy, and thus $\nu L_{syn} \propto t^{-0.3}$ (Chevalier & Fransson 2006b; Maeda 2012b).

In case that the early-phase X-ray was dominated by the IC (which is testable from the late-phase observation as mentioned above), it provides an interesting possibility to probe the electron acceleration mechanism (Chevalier & Fransson 2006b). If there is the spectral flattening, the synchrotron X-ray emission can dominate in the late-phases, and this effect can be identified by the characteristic relatively flat evolution with nearly a constant luminosity ($\propto t^{-0.3}$). If $\gamma_{ff} = 200$, this behavior can be detectable by *Chandra now* (Fig. 3).

5. CONCLUDING REMARKS

In this paper, we have proposed new approaches to investigate the injection and acceleration problem of relativistic electrons at a strong shock wave. A peculiar feature derived from synchrotron radio emissions (in *cm* wavelengths) from nearby young SNe, especially established for stripped-envelope SNe (IIb/Ib/Ic), is the steepness in the intrinsic energy distribution of the radio-emitting relativistic electrons. We suggest this steep distribution could result from a pre-acceleration mechanism able to energize electrons up to the energy threshold needed to start the DSA, as the *cm* emission is produced by electrons whose mean free path is smaller than the shock wave width under the physical conditions realized in young SNe.

According to this interpretation, we suggest that the relativistic electron’s energy distribution could be flattened toward the high energy. We provide an estimate about the energy scale of electrons as ~ 100 MeV (i.e., $\gamma_{ff} \sim 200$) where this could most likely happen. We suggest that identifying (or constraining) this feature can provide an important clue for the still-unresolved electron injection problem, and propose two practically accessible diagnostics on this issue, (1) *mm/sub-mm* ob-

servations in the first one year, and (2) late-time X-ray observations around one year after the explosion or thereafter. The *mm/sub-mm* emission from stripped-envelope SNe is detectable up to ~ 25 Mpc by *ALMA*. The second is applicable up to ~ 10 Mpc by *Chandra*, and currently testable for SN I Ib 2011dh in M51.

Besides investigating the possible flattening of relativistic electrons' distribution, these methods will provide additional information. The *mm/sub-mm* observation can be used to place an independent constraint on the magnetic field strength behind the shock wave. The late-time X-ray observation is able to distinguish the X-ray production mechanism in the early phase. Also, we emphasize the additional uniqueness of the *mm/sub-mm* observation - the transparency even for SNe eI Ib and possibly SNe II p within dense CSM. By combining the *cm* and *mm* observations, both optically thick and thin emissions can be traced to derive physical quantities behind the shock wave (see, e.g., Maeda 2012a). We also note that this transparency increases the applicability of the method to study the shock breakout using the early-phase synchrotron emission (Maeda 2012b), to SNe with

more dense CSM than in *cm*.

Our model prediction is based on the model which explains the *cm* emission from nearby SN cI Ib 2011dh (Maeda 2012a). SN 2011dh is typical among SNe cI Ib/Ib/Ic in its radio properties (Soderberg et al. 2012), and there is a wide distribution of SNe I Ib/Ib/Ic in the synchrotron luminosity (Chevalier et al. 2006a; Chevalier & Soderberg 2010). There are radio strong SNe I Ib/Ib/Ic, more luminous than SN 2011dh by an order of magnitude or even more, including 'engine-driven' SNe sometimes associated with GRBs (Soderberg et al. 2010). For these especially radio strong SNe, the *ALMA* detectable horizon extends even to the greater distance, i.e., ~ 100 Mpc.

This research is supported by World Premier International Research Center Initiative (WPI Initiative), MEXT, Japan. K. M. acknowledges financial support by Grant-in-Aid for Scientific Research for young Scientists (23740141).

REFERENCES

- Bamba, A., Yamazaki, R., Ueno, M., Koyama, K. 2003, ApJ, 589, 827
 Bell, A.R. 1978, MNRAS, 182, 147
 Björnsson, C.-I., & Fransson, C. 2004, ApJ, 605, 823
 Blandford, R.D., & Ostriker, J.P., 1978, ApJ, 221, L29
 Brown, R. L., Wild, W., Cunningham, C. 2004, Advances in Space Research, 34, 555
 Campana, S., & Immler, S. 2012, MNRAS, in press (arXiv:1209.0702)
 Chevalier, R.A. 1998, ApJ, 499, 810
 Chevalier, R.A., Fransson, C., & Nymark, T.K. 2006a, ApJ, 641, 1029
 Chevalier, R.A., & Fransson, C. 2006b, ApJ, 651, 381
 Chevalier, R.A., & Soderberg, A.M. 2010, ApJ, 711, L40
 Ellison, D.C., Berezhko, E.G., Baring, M.G. 2000, ApJ, 540, 292
 Fermi, E. 1949, Phys. Rev., 75, 1169
 Filippenko, A.V., Matheson, T., Ho, L.C. 1993, ApJ, 415, L103
 Filippenko, A.V. 1997, ARAA, 35, 309
 Fransson, C., Lundqvist, P., & Chevalier, R.A. 1996, ApJ, 461, 993
 Fransson, C., & Björnsson, C.-I. 1998, ApJ, 509, 861
 Horesh, A., et al. 2012, submitted to ApJ (arXiv:1209.1102)
 Krauss, M.I., et al. 2012, ApJ, 750, 40
 Maeda, K. 2012a, ApJ, 758, 81
 Maeda, K. 2012b, ApJ, in press (arXiv:1209.1904)
 Margutti, R., et al. 2012, ApJ, 751, 134
 Morlino, G., & Caprioli, D. 2012, A&A, 538, A81
 Nomoto, K., Suzuki, T., Shigeyama, T., Kumagai, S., Yamaoka, H., Saio, H. 1993, Nature, 364, 507
 Sasaki, M., & Ducci, L. 2012, A&A, 546, 80
 Soderberg, A.M., et al. 2010, Nature, 463, 513
 Soderberg, A.M., et al. 2012, ApJ, 752, 78
 Tatischeff, V. 2009, A&A, 499, 191
 Uchiyama, Y., Aharonian, F.A., Tanaka, T., Takahashi, T., Maeda, Y. 2007, Nature, 449, 576
 Woosley, S.E., Eastman, R.G., Weaver, T.A., & Pinto, P.A. 1994, ApJ, 429, 300